TIRF IMAGING OF FOCAL Ca^{2+} RELEASE IN VOLTAGE-CLAMPED ATRIAL AND VENTRICULAR MYOCYTES

Vadim Degtiar, Emily Jones, My Chau, Lars Cleemann, and Martin Morad

Georgetown University, 3900 Reservoir Road, NW, Washington, District of Columbia 20007

Contraction of both atrial and ventricular mammalian cardiomyocytes is controlled by Ca^{2+} signals that are generated by Ca^{2+}-influx via L-type Ca^{2+} channels (DHP-receptors) and amplified by Ca^{2+}-induced Ca^{2+} release (CICR) via Ca^{2+} release channels (ryanodine receptors, RyRs) in the membrane of the sarcoplasmic reticulum (SR). The organization of the SR, however, is quite different: ventricular cells have widely distributed dyadic junctions between SR and t-tubules, while atrial cells, lacking t-tubules, have numerous peripheral couplings at the cell surface and only non-junctional SR and RyR in the cell interior. Confocal measurements of Ca^{2+} sparks have to served to demonstrate functional implications of these structural differences, but has yet to provide a detailed picture in terms of unitary Ca^{2+} fluxes. We have therefore developed a new approach to examine differences in subsarcolemmal Ca^{2+} signaling in atrial and ventricular cells. We use rapid (734 frames/s) total internal reflection fluorescence (TIRF) microscopy, which has the ability to focus on a thin surface layer (~ 0.15 μm) of cells, provided the cells can made to stick to the fluid/glass interface where total internal reflectance takes place.

TIRF microscopy (Axelrod et al., 1982, *J. Microscopy*, 129:19-28) has been used to image structures and events within a surface layer that is considerably thinner ($\Delta z \cong 0.15$ μm) than the depth of the focal plane ($\Delta z \cong 0.8$ μm) provided by other light microscopic techniques, including confocal microscopy. This technique has been used to study surface layers, and fusion of synaptic vesicles. The basic requirement is that is that an exponentially decaying "evanescent" electromagnetic wave is generated at the glass bottom of a perfusion chamber where cells in sufficiently close contact are subject to fluorescence excitation. The evanescent wave arises within an area where a parallel beam through the underlying glass body is totally reflected due to its hypercritical angle of incidence ($\theta > 60^\circ$, $\sin\theta > n_{water}/n_{glass}$, $n_{water} \sim 1.33$, $n_{glass} \sim 1.5$). The glass body in question may be a separate prism on an upright microscope, or, on a more convenient inverted microscope, the objective itself if numerical aperture is sufficient for total internal reflection ($NA > n_{wat}$). Such objectives are now available with NAs of 1.45 to 1.65. We have followed a different approach by designing a system where the first element of a modified Zeiss objective (x40, NA 1.4, oil) combines the geometries of a ball lens and a prism. This allows a compact design, a simple light path, a high angle of incidence (55-80°), and the use of standard optical materials (lens, immersion oil, cover slip). A fiber-coupled laser (HeNe, 10 mW, 488 nm, Omnichrome) was used for fluorescence excitation of Ca^{2+} sensitive dyes (Fluo-3, Fluo-3AM, Fluo-4) and fluorescent beads (0.2 μm Ø). Emitted light (> 500 nm) was intensified (single micro-channel plate) and recorded with fast CCD camera (128x128 pixels, 8 bits, 734 frames/s, Dalsa).

Our general experimental approach was to examine single voltage-clamped cardiomyocytes while simultaneously recording subsarcolemmal Ca^{2+} signals using TIRF

microscopy. Single atrial and ventricular rat cardiomyocytes were prepared for each day of experimentation by enzymatic dissociation of hearts excised rapidly from deeply anestethized rats (*Rattus norvegicus*). The cells were plated onto pretreated glass cover slips (25 mm Ø), and were used within 10 hours. Internally dialyzed cells were voltage-clamped (Dagan) in the whole cell configutation using depolarizing pulses to activate Ca^{2+} current and evoke Ca^{2+} release. The Cs^{+}-based dialyzing solution typically contained 0.8 mM Fluo-4 and 2 mM EGTA.

It is an important property of the TIRF technique that it is sensitive to minute vertical movements (~ 10 nm) within the evanescent field, so that motion artifact might be superimposed on the Ca^{2+} signal that are our primary interest. We therefore studied the development of stable adhesions of cardiomyocytes to pretreated glass cover slip. Variations in pretreatment included different methods of cleaning of the cover slips (waeek acid and/or alcohol), and coating with various compounds (collagen, poly-lysine, gelatin, and laminin) applied in a wetting aqueous solution to provide a final density of (1-20 $\mu g/cm^2$) after drying in a dust free environment at room temperature or ~80 °C. The cells were plated onto the pretreated glass cover slips in different concentration, either immediately after enzymatic dissociation or after stabilizing up to 2 hours, and were then left in Tyrode's solution up to 10 hours. During this period we checked the survival, stickiness, and areas of adhesion of cells. Stickiness was tested by counting the number of cells that remained in position after switching on the stream from a rapid perfusion "puffer" system. The areas of adhesions, and their stability were evaluated in the TIRF mode after staining the cells with the cell permeant Ca^{2+}-indicator dye Fluo-3nAM. We found that a few stable adhesions in each cell developed over a period of hours (>2 h) and had the largest area (5-20 μm across) when the cells where plated immediately after enzymatic dissociation and when laminin was used as coating. Such areas of adhesion had a well-defined outline that did not change when turning on the stream from the puffer or activating contractions by KCl-depolarization. The other compounds (gelatin, collagen, and polysine) did not promote adhesion to the same extent and/or had adverse effects on cell survival. Laminin was effective in a layer (1-2 $\mu g/cm^2$) that is estimated to be too thin (10-20 nm) to degrade the TIRF signals. The methods used for the initial washing of the cover slips and the drying of the coating were of little consequence.

We next proceeded to recorded Ca^{2+} signals in the TIRF mode from voltage clamped cells dialyzed with 0.8 mM Fluo-4 and 2 mM EGTA. Figure 1 compares The Ca^{2+} currents TIRF Ca^{2+} signals recorded in an atrial (panels A-C) and a ventricular cells. The bright field images show outlines and patch electrodes. As shown in panels B and E, cell adhesions appear in TIRF images as relatively small bright areas within the outline of the cells. The smaller bright spots around the cells correspond to fluorescent beads used for focusing on the exact bottom of the perfusion chamber. Panels C and F show the Ca^{2+} currents measured following depolarization to 0 mV in relation to the "global" TIRF Ca^{2+} signals measured at 734 Hz from the entire areas of adhesion. The current in the ventricular cell (panel F) was clearly contaminated by Na^{2+} current, but it was a general finding that Ca^{2+} current in atrial cells was much smaller in atrial than in ventricular cells. Nevertheless, the Ca^{2+} signals, measured as $\Delta F/F_o$, were typically larger in atrial cellsthan in ventricular cells and developed developed faster as indicated by the arrows at 50% of peak (10 vs. 15 ms). This finding may indicate that the peripheral couplings in atrial cells are located within reach of the evanescent wave, while Ca^{2+} from dyadic releases in ventricular cells reach the cell surface only after some diffusion delay.

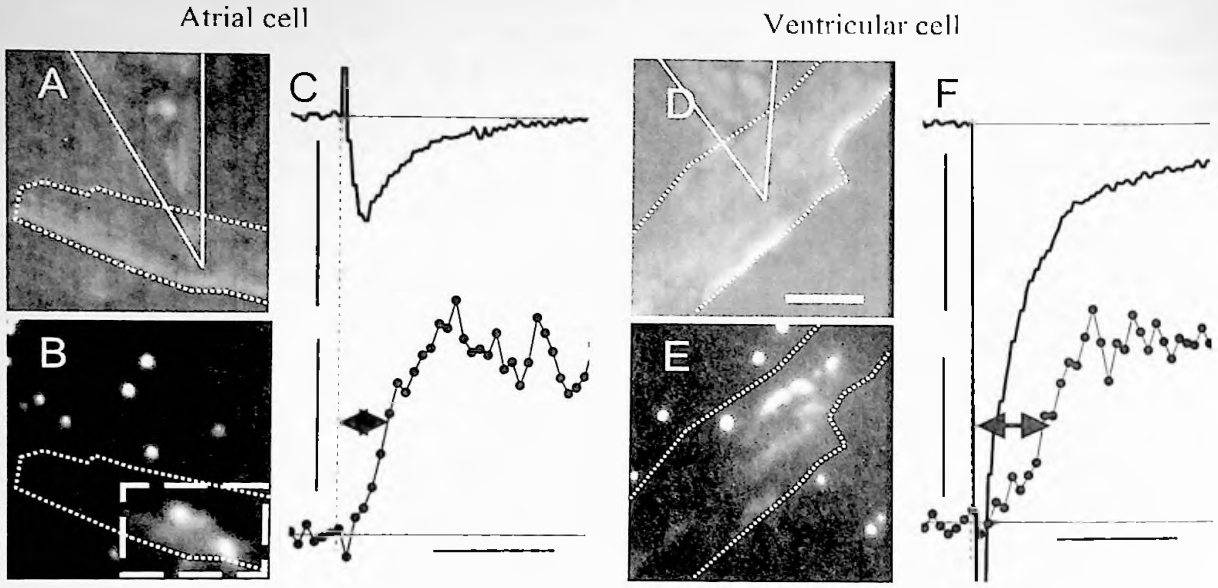

Figure1. Comparison of TIRF Ca signals in voltage clamped atrial (panels A-C) and ventricular (panels D-E) cells. Panels A and D show bright field images with outlines of the cells and the patch electrodes. The outlines of the cells were transferred to panels B and E, which show the areas of adhesion within the cells and several fluorescent beads mainly around the cells. The box in panel B corresponds to the area analyzed in Fig. 2. Panels C and F show recorded Ca^{2+} currents (top) and the glabal TIRF Ca^{2+} signals measured within the entire area of adhesion. The scale bars in panels C and D correspond to 1000 pF for the current trace, 0.5 (panel B) or (0.3) panel (F) for the Ca^{2+} signal, and 20 ms for the common time axis. The atrial cell was depolarized from –60 to 0 mV while the ventricular cell was depolarized from –80 to 0 mV.

When examined in greater details, the ca signals within the areas of adhesion showed distinct patterns. Figure 2 shows consecutive frames recorded at 1.4 ms intervals in an atrial cell (the same as in Fig. 1A-C) immediately after depolarization (#1-5) and ~15 m later (#12). Notice that bright fluorescence spots appear in increasing numbers from one frame to the next. The regularly spaced arrows in frame # 3 point at focal Ca^{2+} signals that appeared on a longitudinal line with the approximate sarcomere spacing (~ 1.8 μm). This longitudinal alignment was also noticeable at a later time (frame #12) when the patter of focal Ca^{2+} signals is much denser. It was also common to observe to bserve Ca signal aligned in the transverse direction (#12). Some prominent focal Ca^{2+} signals can clearly be followed from frame to frame (vertical arrows in frames #3-5) yet do not last nearly as long as the typical Ca sparks (~15-20 ms duration in observed with confocal microscopy (vertical arrows in frames #3-5) yet do not last nearly as long as the Ca^{2+} sparks typically observed with confocal microscopy (~15-20 ms in rat atrial cardiomyocytesmycytes). It should be noticed, however that we also detected longer lasting focal Ca^{2+} signal resembling the focal Ca releases observed with confocal microscopy.

Our results acquired with TIRF microscopy, suggest that Ca^{2+} signaling in the subsarcolemmal spaces of atrial and ventricular myocytes, in addition to the conventional Ca^{2+} sparks, described by confocal microscopy, is accompanied by brief, focal events. These brief events, possibly "quarks", appear to reactivate at the same location, unlike the sparks, and often

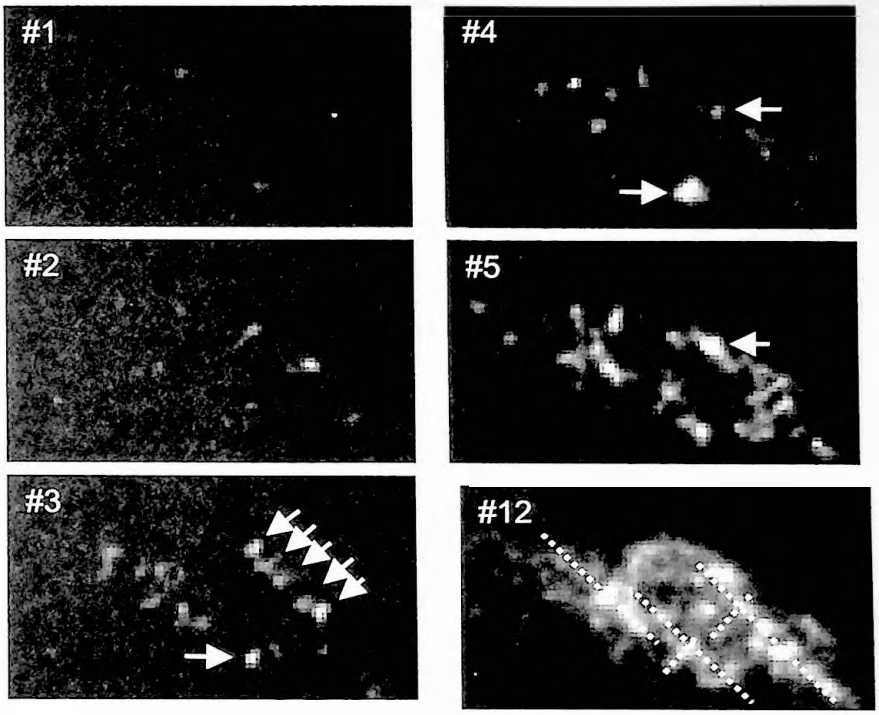

Figure 2. Focal Ca^{2+} releases recorded 7in the TIRF mode at 734 Hz immediately after voltage-clamp depolarization of an atrial cardiomyocyte from –60 to 0 mV. The frames #1-5 are numbered consecutively each showing the light accumulated during a 1.4 ms interval. Frame #12 was recorded near the peak of the global Ca^{2+} signal about 18 ms after depolarization and is reproduced with a different gray scale. Arrows and lines indicate prominent focal Ca^{2+} signals and their spacing and alignment.

trigger other adjacent (within 1-2 μm) fast events. The probability of both very fast, and "classical" Ca^{2+} events was markedly increased (comparing to the probability of spontaneous events occurring at –80 or –60 mV) already with moderate depolarizations (-50 to –30 mV), and further increased at 0mV. However, very strong depolarizations (+80 mV) only slightly supported subsarcolemmal Ca^{2+} signaling, with a very strong signal triggered by the tail-current during membrane repolarization.

In addition to an increase of probability of transient events to occur, depolarization also caused a steady elevation of Ca^{2+} concentration. The very fast and brief events were also seen in experiments where cells were dialyzed with internal solution containing only Fluo-4, without other exogenous Ca^{2+} buffers. Addition of EGTA reduced mainly the overall accumulation of Ca^{2+} in subsarcolemmal space. I.e., the relative slow increase of (F/Fo) during prolonged depolarization was dramatically stronger in experiments with low or no exogenous Ca^{2+} -buffers added to the internal solution, while transient events were affected to a lesser extent. Despite the smaller Ca^{2+} channel current density, atrial myocytes revealed stronger changes in the subsarcolemmal $[Ca^{2+}]$, compared to ventricular ones.

We conclude that TIRF microscopy provides detailed information about the subsarcolemmal Ca^{2+} signaling, that appear to be different isn atrial and ventricular myocytes. The high spatial and temporal resolution of the techniqe reveal in fascinating details a new level of Ca^{2+} signaling. The detailed analysis of these Ca^{2+} signals in terms of the Ca^{2+} fluxes generated by clustered or single DHP- and RyRs remains to be performed. Supported by AHA 9808116U and NIH RO1 16152.